



In vivo assessment of extracellular pH of joint tissues using acidoCEST-UTE MRI

Rachel A. High^{1,2#}, Yang Ji^{1#}, Ya-Jun Ma¹, Qingbo Tang^{1,2}, Mark E. Murphy³, Jiang Du^{1,2}, Eric Y. Chang^{1,2}

¹Department of Radiology, University of California, San Diego Medical Center, San Diego, CA, USA; ²Research Service, ³Orthopedic Surgery Service, VA San Diego Healthcare System, San Diego, CA, USA

#These authors contributed equally to this work.

Correspondence to: Rachel A. High, PhD. University of California, San Diego Medical Center, San Diego, CA, USA. Email: rachelahigh@gmail.com.

Background: Degradation of cartilage and meniscus may be mediated by changes in extracellular pH. The purpose of this study was to optimize saturation powers used with the acidoCEST magnetic resonance imaging (MRI) technique with a 3D ultrashort echo time readout (acidoCEST-UTE) and to demonstrate feasibility of the method for measuring pH in cartilage and meniscus *in vivo*.

Methods: Magnetization transfer ratio asymmetry and ratio of radiofrequency (RF) power mismatch at different powers were evaluated in cartilage and meniscus tissue phantoms for iopamidol and iohexol. Using optimized RF powers, the acidoCEST-UTE MRI sequence was used to assess pH of joint fluid and tissues in four patients after direct intra-articular administration of iodinated contrast.

Results: In the phantoms, the ratio of powers 0.54/1.10 μ T showed the strongest correlation with pH. *In vivo* acidoCEST-UTE pH measurements of intra-articular fluid were similar to electrode measurements of the contrast agent (7.22 *vs.* 7.1 for iopamidol, respectively; 7.65 *vs.* 7.5 for iohexol, respectively). As measured with the acidoCEST-UTE technique, overall mean cartilage pH was significantly lower than overall mean meniscus pH (6.60 *vs.* 6.72, respectively; $P=0.043$).

Conclusions: AcidoCEST-UTE MRI after direct intra-articular administration of either iopamidol or iohexol can be used to measure cartilage and meniscus pH *in vivo*.

Keywords: AcidoCEST-MRI; chemical exchange saturation transfer ultrashort echo time (CEST UTE); osteoarthritis; pH; acidosis

Submitted Jun 16, 2019. Accepted for publication Aug 14, 2019.

doi: 10.21037/qims.2019.08.11

View this article at: <http://dx.doi.org/10.21037/qims.2019.08.11>

Introduction

Osteoarthritis is a debilitating disease with considerable individual and societal impact (1). Progression of this disease is mediated by a variety of biochemical factors. One such factor, extracellular pH, affects expression and function of several proteins involved in the degradation of cartilage (2,3). In particular, chondrocytes, which are responsible for synthesis and maintenance of the cartilage matrix, have been shown to exhibit inhibited matrix synthesis in acidic conditions (pH<7.1) (4). Certain cells present in the

environment of the joint are even able to modulate pH, such as osteoclasts, which dissolve bone by secretion of acid (5). In addition to driving cartilage degradation, the acidification of joint tissue may contribute to osteoarthritis-related pain. Decreased pH in neuromusculoskeletal structures has been correlated with increased pain (6-9), and thus could help explain the poor association between patient-reported pain and degenerated structural findings on magnetic resonance imaging (MRI) (10).

Until recently, pH of cartilage and meniscus could only be measured *ex vivo*, or *in vivo* by an invasive process. Now,

non-invasive, pH-sensitive measurements can be made with chemical exchange saturation transfer (CEST) MRI, or acidoCEST MRI (11,12). This technique uses Food and Drug Administration- and European Medicines Agency-approved diamagnetic contrast agents, such as iopamidol or iohexol, to measure the exchange of protons between water and amide side chains. While acidoCEST MRI has predominantly been used to measure pH in tumors, the technique has recently been modified by Ma *et al.* (13) for application to musculoskeletal tissues. Traditional acidoCEST sequences have long, high-power saturation periods and use readouts with longer echo times (14), which are not suitable for tissues with short T2 relaxation such as cartilage and meniscus (15). This barrier has been overcome by the addition of an ultrashort echo time (UTE) readout to the acidoCEST sequence (16). Still, acidoCEST-UTE sequence parameters remain unoptimized for musculoskeletal tissues and the technique has not yet been applied to patients for measurement of pH in musculoskeletal tissues *in vivo*. Previous work by Ma *et al.* determined that ratio of radiofrequency power mismatch (RPM) showed strong correlation coefficients between fluid, cartilage, and meniscus, yet only two saturation powers, 0.56 and 1.10 μT , were evaluated. As CEST effect is saturation power-dependent (17), additional powers should be tested for optimal performance.

The purpose of this study was to optimize saturation powers used with the acidoCEST-UTE MRI technique in phantoms and demonstrate feasibility of measuring *in vivo* pH of intra-articular structures, including cartilage and meniscus. First, multiple saturation powers between 0.54 and 1.30 μT were evaluated in fluid and tissue phantoms for both iopamidol and iohexol. Second, the powers whose RPM showed the strongest correlation coefficients between fluid, cartilage, and meniscus were selected for use *in vivo*.

Methods

Chemicals

Stock solutions of 972 mM iopamidol (370 mgI/mL Isovue; Bracco Imaging S.p.A, Milan, Italy) and 920 mM iohexol (350 mgI/mL Omnipaque; GE Healthcare, Chicago, IL, USA) were commercially purchased for use in this study. All other chemicals were purchased from Sigma-Aldrich (St. Louis, MO).

Phantom preparation

A set of *ex vivo* cartilage and meniscus samples was prepared

with either iopamidol or iohexol at 200 mM concentration and phosphate-buffered saline (PBS) at 10 mM final concentration. Samples were harvested from grossly normal tissues, from two male donors aged 48 and 88. Coins of pure cartilage from osteochondral cores and menisci slices were created from various locations in the joint. Tissues were soaked in buffered contrast agent solution for 24 hours and sealed in plastic syringes prior to scanning. Solution pH values ranged between 6.19 and 7.8 and were tested before and after scanning to ensure pH stability. Phantoms were bundled in a cylindrical container, filled with Fomblin (Ausimont, Thorofare, NJ), and scanned parallel to B_0 at isocenter. Phantoms were maintained at physiologic temperature (35 ± 0.2 °C) during scanning by an MRI-compatible, regulated air heater, which was made in-house.

Human subjects

The studies were conducted under an approved Institutional Review Board protocol at the VA San Diego Healthcare System and signed, informed consent was obtained from all participants. Four male subjects (mean age 56 years, range 46–63 years) were recruited, ranging in symptoms from asymptomatic to severe, chronic knee pain. Standard, sterile techniques were employed, and for each patient a 20 gauge 1.5” needle was inserted into the knee joint through an anterior approach under fluoroscopic imaging guidance. Approximately 35 cc of contrast was injected into the joint (n=2, iopamidol 370 mgI/mL; n=2, iohexol 350 mgI/mL). After contrast injection, patients were asked to engage in light walking to encourage contrast to permeate the tissue. MR imaging was performed between 1 and 6.5 hours after injection. In two of the four subjects, contrast-agent bottles used for intra-articular injection were tested with a calibrated pH electrode (LE422, FiveEasy F20 bench meter; Mettler Toledo, Columbus, OH).

Magnetic resonance imaging

MRI scanning was performed on a 3T clinical MRI scanner (MR750, GE Healthcare, Milwaukee, WI) using an 8-channel transmit/receive knee coil. The CEST pulse sequence used in this study consists of a frequency selective Fermi saturation pulse (duration =32 milliseconds, bandwidth =40 Hz) followed by the acquisition of a 3D ultrashort echo time (UTE) cones sequence. For the *ex vivo* cartilage and meniscus phantom scans, the CEST imaging parameters were as follows: TR =62 ms, TE

=0.032 ms, number of spokes (Nsp) =5, spoke interval (τ) =5 ms, flip angle (FA) =5°, bandwidth (BW) =166 kHz, field of view (FOV) =12×12×11.2 cm³, and matrix size =160×160×28. Z-spectra were acquired at varying saturation offset frequencies from -1,080 Hz to 1,080 Hz with 40 Hz steps using saturation pulses with B1 of 0.54, 0.65, 0.97, 1.10, and 1.30 μ T (300°, 360°, 540°, 600°, and 720° respectively) as calculated by power average. The scanning time of each frequency was 1 minute and 10 seconds. For *in vivo* scanning, the sequence parameters were identical to the *ex vivo* phantom scans except for higher resolution (FOV =12×12×11.2 cm³, and matrix size =160×160×28) and resultant 2-minute scan time per frequency. CEST images were acquired at varying saturation offset frequencies from \pm 430 to \pm 670 Hz with a step size of \pm 40 Hz using saturation pulses with B1 of 0.54 and 1.10 μ T (300° and 600°). Acquisitions were interleaved (e.g., +/- ppm and 0.54/1.10 μ T powers for each offset were paired). High in-plane resolution T2-weighted images were acquired using a 3D fast-spin echo (FSE) sequence for both *ex vivo* and *in vivo* studies to enhance the contrast of tissue and improve the accuracy of drawing ROIs. A dual-echo UTE sequence with two echo times (TE1 =0.032 ms; TE2 =2.2 ms) was performed to generate a ΔB_0 map, which was used for B₀ correction for CEST data processing. Total *in vivo* scanning time was ~60 minutes.

Data processing

All data were processed in MATLAB (Mathworks, Natick, MA). All images were smoothed using a 3D Gaussian kernel with standard deviation of 0.8 to remove noise. The dual echo time method calculates the ΔB_0 maps from the difference of two gradient echo-based phase images acquired at TE₁ and TE₂:

$$\Delta B_0 = \frac{\Delta\Phi}{\gamma \cdot \Delta TE} = \frac{\Phi_{TE_2} - \Phi_{TE_1}}{\gamma \cdot (TE_2 - TE_1)} \quad [1]$$

where Φ_{TE_i} is the phase image acquired at echo time TE_i using 3D UTE cones sequence, and γ is the gyromagnetic ratio for hydrogen, ¹H.

The CEST images with different frequency offsets were interpolated using the spline method to generate images with a fine increment of 0.015 ppm. B₀-corrected CEST images at \pm 4.2, \pm 4.3, or \pm 5.6 ppm were obtained from the interpolated CEST images by selecting signals according to the frequency shift in ΔB_0 map pixel by pixel.

The magnetization transfer ratio asymmetry (MTR_{asym})

was calculated by:

$$MTR_{asym} = \frac{I(-\Delta\omega) - I(\Delta\omega)}{I_0} \quad [2]$$

where $\Delta\omega$ is the frequency offset of mobile protons with respect to bulk water resonance at 0 ppm. $I(-\Delta\omega)$ and $I(\Delta\omega)$ are the signal intensities with saturation pulse at $+\Delta\omega$ and $-\Delta\omega$, respectively. I_0 is the signal intensity with no saturation pulse.

RPM was determined by comparing MTR_{asym} index which was obtained under two RF saturation power from a single labile proton group in contrast agent:

$$RPM = \frac{[(1 - MTR) / MTR]_{RF1}}{[(1 - MTR) / MTR]_{RF2}} \quad [3]$$

where subscript RF1 and RF2 indicate the different RF irradiation powers for MTR_{asym} index.

ROI selection and pH calculation

MTR_{asym} maps were created by masking for positive values (e.g., pixels where MTR_{asym} <0 were excluded) and increasing values at higher powers (e.g., pixels where MTR_{asym} at 0.56 μ T > MTR_{asym} at 1.10 μ T were excluded) to threshold against noise. Masked MTR_{asym} pixel maps were evaluated by a musculoskeletal radiologist and intra-articular structures and locations with maximal values (indicating greatest contrast accumulation) were noted. Thereafter, using the I₀ image, a second scientist drew ROIs on these structures for pH calculation. Pixel maps of pH were generated using the equation of the line of best fit for the iopamidol and iohexol fluid and tissue phantoms. For the iopamidol phantom, the best fit line for RPM (0.56/1.10 μ T) and pH yielded the equation:

$$y = 1.88x - 10.21 \quad [4]$$

where y is RPM and x is pH. For the iohexol phantom, the equation from Ma *et al.* (13) was used:

$$y = 1.56x - 8.39 \quad [5]$$

Statistical analysis

Statistical analyses were performed using the SPSS software package (v. 21; SPSS, Chicago, IL). The Shapiro-Wilk test was used to assess normality. Descriptive statistics were performed. Correlations between pH and RPM calculated using various powers were performed in the phantoms. Student's *t*-test was performed to compare mean pH values of cartilage and menisci *in vivo*. A P value less than 0.05 was

considered statistically significant.

Results

For the phantoms containing 200 mM iopamidol or iohexol and samples of *ex vivo* meniscus and cartilage, a comparison of the z-spectra (Figure 1) demonstrated that the CEST effect of these agents change as saturation power increases from 0.54 to 1.30 μT , in fluid (Figure 1A,G), meniscus (Figure 1B,H), and cartilage (Figure 1C,D). In general, MTR_{asym} increased with increasing power for fluid, meniscus, and cartilage using either iopamidol or iohexol. RPM of iopamidol at 4.2 ppm and iohexol at 4.3 ppm was calculated for power ratios 0.54/1.10, 0.65/0.97, 0.65/1.30, and 0.97/1.30 μT , over a pH range of 6.2 to 7.8 for fluid (Figure 1D,J) as well as meniscus (Figure 1E,K) and cartilage (Figure 1F,L). In meniscus and cartilage, the RPM calculated with saturation powers of 0.54 and 1.10 μT yielded the most consistently linear relationship with pH and thus these were selected as the powers to be used *in vivo*. For iohexol at 4.3 ppm, $R^2=0.96$ and 0.91 for meniscus and cartilage, respectively, and for iopamidol at 4.2 ppm, $R^2=0.76$ and 0.75 for meniscus and cartilage, respectively.

Figure 2 demonstrates representative images from a 55-year-old man, injected with ~35 cc of undiluted iopamidol, and imaged 2-hours post injection. MTR_{asym} could be detected in the cartilage of the medial femoral condyle at the weight-bearing aspect and anterior horn of the medial meniscus. Accumulation of the injected fluid in the suprapatellar recess is evident on the proton-density weighted image (Figure 2A). Average MTR_{asym} of the intra-articular fluid was 0.03 at 0.54 μT (Figure 2D) and 0.08 at 1.10 μT (Figure 2G). Average RPM for the same fluid ROI (Figure 2J) was calculated to be 3.37. Using Eq. [4], this corresponds to an average pH of 7.22. The batch of iopamidol was pH tested post-injection with an electrode and confirmed as pH 7.1. The pH of each pixel in the fluid ROI is shown in Figure 2M. The anterior horn of the medial meniscus (Figure 2B) demonstrated an MTR_{asym} value of 0.05 at 0.54 μT (Figure 2E) and 0.14 at 1.10 μT (Figure 2H). Average RPM for this meniscus ROI (Figure 2K) was 2.82, corresponding to an average pH of 6.93. The pH of each pixel in the meniscus ROI is shown in Figure 2N. An ROI over the cartilage of the medial femoral condyle (Figure 2C) had an MTR_{asym} value of 0.03 at 0.54 μT (Figure 2F) and 0.06 at 1.10 μT (Figure 2I). Average RPM for this cartilage ROI (Figure 2L) was 2.20, corresponding to an average pH of 6.60. The pH of each pixel in the cartilage ROI is shown in

Figure 2O.

Figure 3 shows representative images from a 46-year-old man injected with ~35 cc of undiluted iohexol and imaged at 1-hour post injection. MTR_{asym} could be detected in the cartilage of the femoral trochlea and in an incidentally noted discoid lateral meniscus. Iohexol fluid accumulation is present in the suprapatellar recess (Figure 3A). This fluid MTR_{asym} was 0.03 at 0.54 μT (Figure 3D) and 0.11 at 1.10 μT (Figure 3G). Average RPM for the same fluid ROI (Figure 3J) was 3.54. Using Eq. [5], this RPM value corresponds to an average pH of 7.65. The bottle of iohexol used was pH tested with an electrode at pH 7.5 after injection. The pH of each pixel in the fluid ROI is shown in Figure 3M. The intact discoid lateral meniscus (Figure 3B) demonstrated an MTR_{asym} of 0.04 at 0.54 μT (Figure 3E) and 0.09 at 1.10 μT (Figure 3H). Average RPM for the same meniscus ROI (Figure 3K) was 2.54, or pH 7.00. The pH of each pixel in the meniscus ROI is shown in Figure 3N. Femoral trochlear cartilage (Figure 3C) MTR_{asym} was 0.03 at 0.54 μT (Figure 3F) and 0.05 at 1.10 μT (Figure 3I). Average RPM for the same cartilage ROI (Figure 3L) was 2.09, or pH 6.74. The pH of each pixel in the cartilage ROI is shown in Figure 3O.

In total, 18 ROIs were identified in cartilage and 25 ROIs were identified in meniscus on all the exams. Overall average pH values for all cartilage and meniscus ROIs for both iopamidol and iohexol are given in Table 1. Student's *t*-test showed that overall mean cartilage pH was significantly lower than overall mean meniscus pH (6.60 *vs.* 6.72, respectively; $P=0.043$).

Discussion

In this study, we utilized the acidoCEST-UTE technique to measure cartilage and meniscus tissue pH. We first assessed the effect of saturation power in phantoms, ranging from 0.54 to 1.30 μT , and determined that RPM calculated from a combination of 0.54 μT (300°) and 1.1 μT (600°) yielded the strongest correlation with electrode measured pH. We also demonstrated feasibility of the technique for measuring pH in musculoskeletal tissue *in vivo* on a clinical 3 T scanner.

Direct intra-articular injection of iopamidol or iohexol is a safe, minimally invasive, and routinely performed procedure in clinical practice. This procedure is typically used in smaller volumes to confirm intra-articular access for steroid injections or in larger volumes (>35–50 cc) to highlight internal derangement (18). We demonstrate that

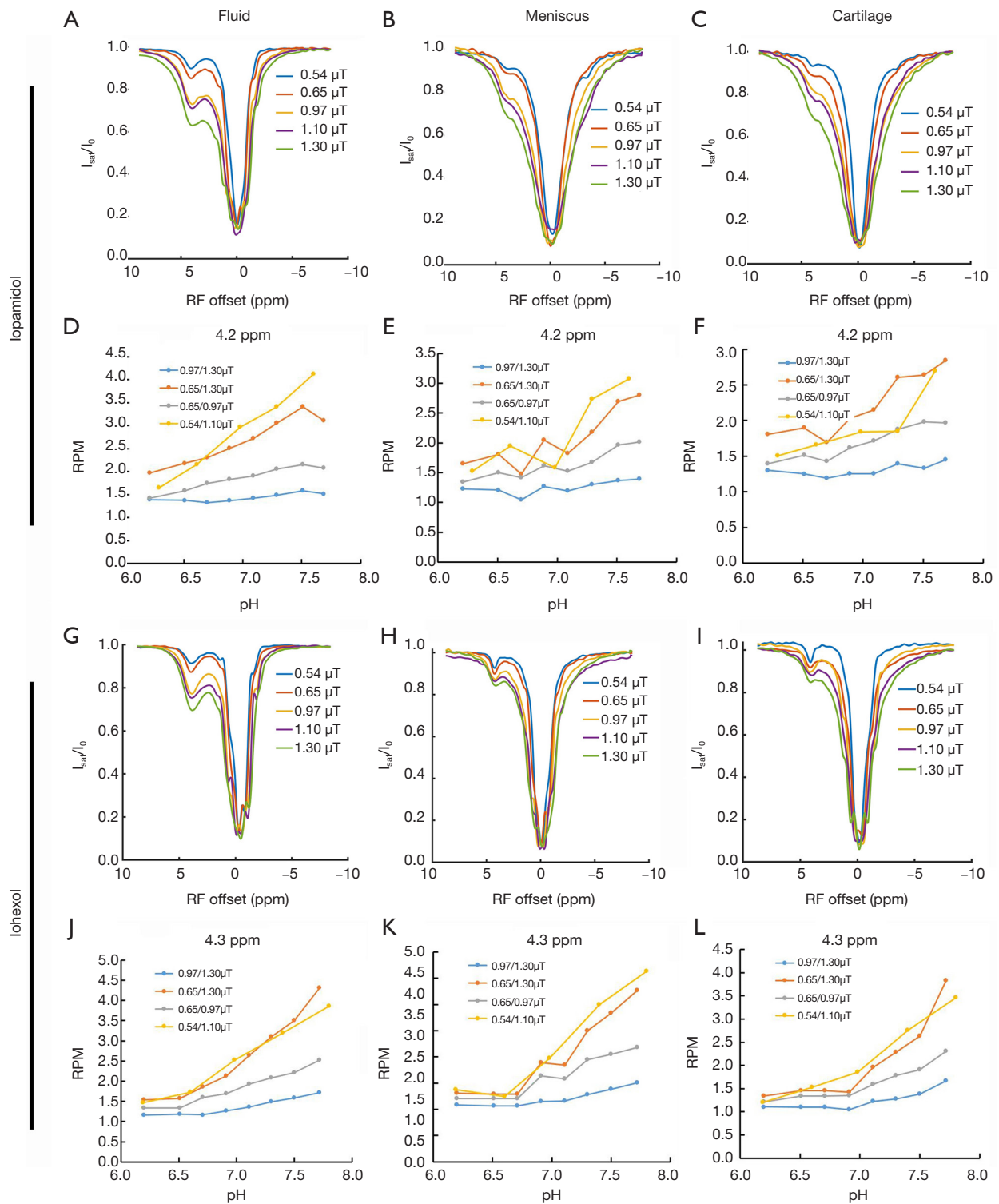


Figure 1 Z-spectrum and RPM maps of iopamidol and iohexol in tissue phantoms at pH 6.2 to 7.8. The first two rows are the z-spectra for fluid (A), meniscus (B), and cartilage (C), and RPM values for fluid (D), meniscus (E), and cartilage (F) for iopamidol at 4.2 ppm. The second two rows are the z-spectra for fluid (G), meniscus (H), and cartilage (I), and RPM values for fluid (J), meniscus (K), and cartilage (L) for iohexol at 4.3 ppm. RPM, radiofrequency power mismatch.

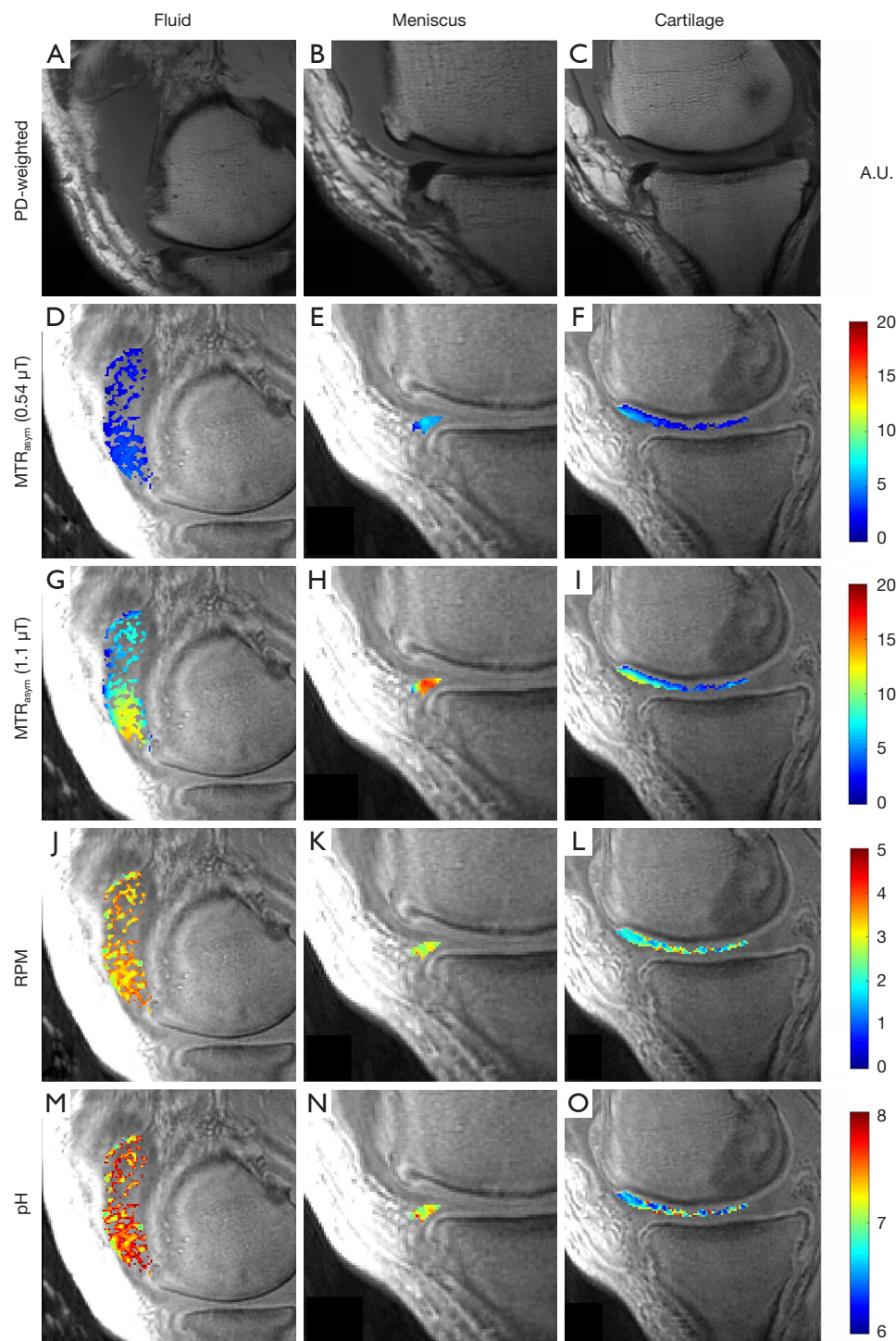


Figure 2 Representative images of fluid, meniscus, and cartilage after intra-articular administration of iopamidol in a 55-year-old man with moderate symptomatic osteoarthritis. The first column shows a PD-weighted image of a region of fluid accumulation in the suprapatellar recess (A) and corresponding parametric maps of MTR_{asy} at 0.54 μT (D) and 1.10 μT (G), RPM (J), and pH (M) for the same region. The second column shows a PD-weighted image of a section of medial meniscus (B), corresponding MTR_{asy} at 0.54 μT (E) and 1.10 μT (H), RPM (K), and pH (N). The third column shows a PD-weighted image of a section of cartilage (C), corresponding MTR_{asy} at 0.54 μT (F) and 1.10 μT (I), RPM (L), and pH (O). PD, proton density; MTR_{asy} , magnetization transfer ratio asymmetry; RPM, radiofrequency power mismatch.

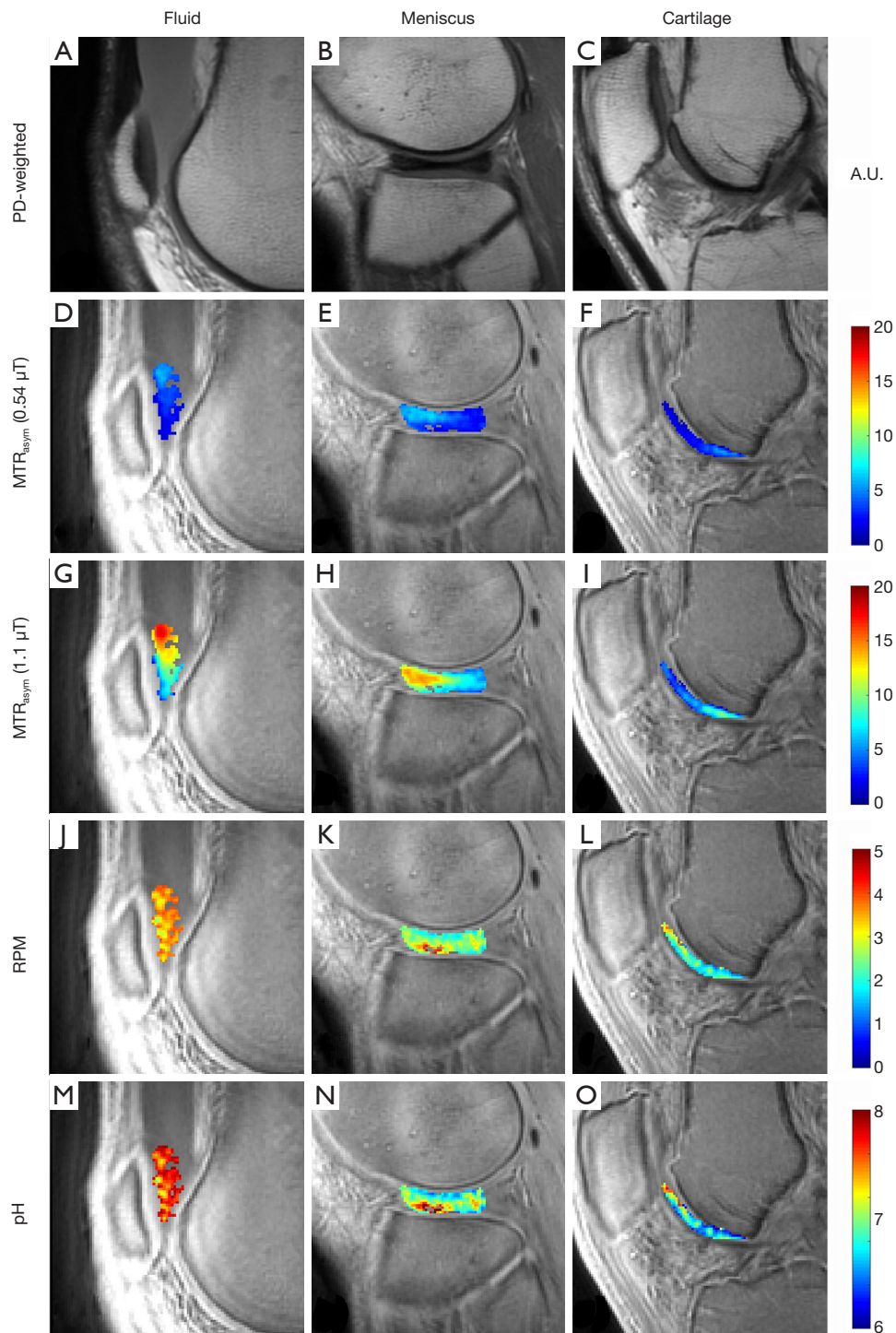


Figure 3 Representative images of fluid, meniscus, and cartilage after intra-articular administration of iohexol in a 46-year-old man with occasional knee pain. The first column shows a PD-weighted image of a region of fluid accumulation in the suprapatellar recess (A) and corresponding parametric maps of MTR_{asym} at 0.54 μT (D) and 1.10 μT (G), RPM (J), and pH (M) for the same region. The second column shows a PD-weighted image of a discoid lateral meniscus (B), with corresponding MTR_{asym} at 0.54 μT (E) and 1.10 μT (H), RPM (K), and pH (N). The third column shows a PD-weighted image of a section of cartilage (C), corresponding MTR_{asym} at 0.54 μT (F) and 1.10 μT (I), RPM (L), and pH (O). PD, proton density; MTR_{asym} , magnetization transfer ratio asymmetry; RPM, radiofrequency power mismatch.

Table 1 *In vivo* pH values and standard deviations of cartilage and meniscus

Tissue	Iopamidol		Iohexol	
	Number of ROIs	Average pH	Number of ROIs	Average pH
Cartilage	5	6.54±0.05	13	6.60±0.17
Meniscus	5	6.65±0.11	20	6.72±0.16

sufficient contrast agent is present between 1 and 6.5 hours after administration to detect a CEST effect and measure tissue pH with the acidoCEST-UTE technique.

Compared with anionic contrast agents previously used with direct arthrography, non-ionic agents such as iopamidol and iohexol diffuse equally into normal and degenerated cartilage samples (19). This property makes iopamidol and iohexol ideal acidoCEST agents, as strong CEST effects should be able to be detected regardless of tissue integrity. The passage of non-ionic iodinated contrast into the cartilage and menisci occurs through a combination of diffusion and convection (bulk flow). Diffusion is strongly influenced by molecular size (20) and, based on this, it would be expected that iopamidol would diffuse into tissues better than iohexol (777.1 vs. 821.1 g/mol, respectively). This is supported by our results which show higher MTR_{asym} values with iopamidol. However, diffusion/convection into intra-articular tissues such as cartilage and menisci occurs simultaneously as synovial resorption and extra-articular diffusion of contrast (20). Diffusion of contrast into the tissue may potentially be improved with increased range of motion. Entezari *et al.* (21) demonstrated that mechanical convection increased the contrast concentration in cartilage tissues by 71% at 30 minutes. Our results support this idea, in that the weightbearing aspects of the femoral condyles preferentially showed detectable MTR_{asym} values. In addition, the discoid lateral meniscus in one of our patients showed diffusely increased MTR_{asym} values (Figure 3E,H), consistent with the fact that discoid menisci are subject to greater stresses compared with regular menisci (22). Although our subjects were instructed to mobilize after injection (i.e., walk around), in the future we will recommend motions with greater range to improve mechanical convection. Higher degrees of flexion will increase the load at the posterior-most portion of the condyles as well as the patellofemoral contact. Flexion increases load transmission through the menisci to 85–90%, compared to 50–70% in extension (23).

Our results show that both cartilage and meniscus are slightly acidic. It is generally accepted that the negative fixed charge density of proteoglycans causes proton attraction, reducing extracellular pH, as evident by the acidic range of all previously reported values (<7.1) (24,25). However, there is debate as to the direction of pH change in diseased cartilage. Experiments by Gray *et al.* (24) strongly suggest that pH follows matrix fixed-charge density (e.g., compressive loading, which leads to greater negative fixed charge density causes an acidic shift). This would suggest that cartilage degradation, where proteoglycans are decreased, would result in a basic shift. Kontinen *et al.* (2), however, found that diseased cartilage is more acidic compared with more normal cartilage. We aim to clarify this in future investigations of *in vivo* pH measurement with the acidoCEST-UTE technique. To the best of our knowledge, pH measurements of menisci have not been previously performed. However, menisci have lower amounts of proteoglycan compared with articular hyaline cartilage (15), and based on the above results from Gray *et al.* (24) we would expect a higher (more basic) pH compared with cartilage, which is confirmed by our experimental results.

There are several limitations to our study. First, ours was a feasibility study with small sample size. However, *in vivo* assessment of tissue pH in the joint has not been performed previously. This study serves as a proof-of-concept with pilot results that are encouraging enough to continue the technique in larger sample sizes with future aims of elucidating the relationship between tissue pH and degradation or patient pain. Second, although we investigated various saturation powers, the imaging protocol remains suboptimal for clinical application. A relatively long scan time (~60 minutes) contributed to motion artifacts. Future experiments will explore opportunities for scan acceleration, including fewer acquisitions (e.g., fewer off-resonance datapoints), improvements in the UTE sequence (e.g., optimization of spokes acquired per TR), smaller scan coverage centered on the structures of interest, and implementation of advanced acceleration techniques such as compressed sensing or parallel imaging (26,27). Third, MTR_{asym} was not able to be detected in several regions of cartilage and meniscus. Although we had an insufficient sample size for formal analysis, we subjectively noted that greater regions of tissue contrast accumulation were present in patients imaged closer to 1–2 hours after injection. As mentioned above, we also believe that increased patient range of motion after injection will improve mechanical convection and provide detectable contrast in more regions

throughout the joint in future studies.

In conclusion, measuring *in vivo* musculoskeletal tissue such as cartilage and meniscus using acidoCEST-UTE MRI is feasible. Both iopamidol and iohexol appear to be suitable contrast agents for this purpose.

Acknowledgments

Funding: The authors gratefully acknowledge grant support from the VA Rehabilitation Research and Development Service (Merit Award I01RX002604), VA Clinical Science Research and Development Service (Merit Award I01CX001388), and NIH (1R01AR075825, 1R21AR073496, 5R01AR062581, and 1R01NS092650).

Footnote

Conflicts of Interest: The authors have no conflicts of interest to declare.

Ethical Statement: The studies were conducted under an approved Institutional Review Board protocol at the VA San Diego Healthcare System and signed, informed consent was obtained from all participants.

References

- Hunter DJ, Schofield D, Callander E. The individual and socioeconomic impact of osteoarthritis. *Nat Rev Rheumatol* 2014;10:437-41.
- Kontinen YT, Mandelin J, Li TF, Salo J, Lassus J, Liljeström M, Hukkanen M, Takagi M, Virtanen I, Santavirta S. Acidic cysteine endoprotease cathepsin K in the degeneration of the superficial articular hyaline cartilage in osteoarthritis. *Arthritis Rheum* 2002;46:953-60.
- Razaq S, Wilkins RJ, Urban JPG. The effect of extracellular pH on matrix turnover by cells of the bovine nucleus pulposus. *Eur Spine J* 2003;12:341-9.
- Wilkins RJ, Hall AC. Control of matrix synthesis in isolated bovine chondrocytes by extracellular and intracellular pH. *J Cell Physiol* 1995;164:474-81.
- Blair HC. How the osteoclast degrades bone. *BioEssays* 1998;20:837-46.
- Issberner U, Reeh PW, Steen KH. Pain due to tissue acidosis: a mechanism for inflammatory and ischemic myalgia? *Neurosci Lett* 1996;208:191-4.
- Izumi M, Ikeuchi M, Ji Q, Tani T. Local ASIC3 modulates pain and disease progression in a rat model of osteoarthritis. *J Biomed Sci* 2012;19:77.
- Deval E, Lingueglia E. Acid-sensing ion channels and nociception in the peripheral and central nervous systems. *Neuropharmacology* 2015;94:49-57.
- Sugimura N, Ikeuchi M, Izumi M, Kawano T, Aso K, Kato T, Ushida T, Yokoyama M, Tani T. Repeated intra-articular injections of acidic saline produce long-lasting joint pain and widespread hyperalgesia. *Eur J Pain* 2015;19:629-38.
- Yusuf E, Kortekaas MC, Watt I, Huizinga TWJ, Kloppenburg M. Do knee abnormalities visualised on MRI explain knee pain in knee osteoarthritis? A systematic review. *Ann Rheum Dis* 2011;70:60-7.
- Chen LQ, Howison CM, Jeffery JJ, Robey IF, Kuo PH, Pagel MD. Evaluations of extracellular pH within in vivo tumors using acidoCEST MRI. *Magn Reson Med* 2014;72:1408-17.
- Ji Y, Zhou IY, Qiu B, Sun PZ. Progress toward quantitative in vivo chemical exchange saturation transfer (CEST) MRI. *Isr J Chem* 2017;57:809-24.
- Ma YJ, High RA, Tang Q, Wan L, Jerban S, Du J, Chang EY. AcidoCEST-UTE MRI for the assessment of extracellular pH of joint tissues at 3 T. *Invest Radiol* 2019;54:565-71.
- Jones KM, Randtke EA, Howison CM, Pagel MD. Respiration gating and Bloch fitting improve pH measurements with acidoCEST MRI in an ovarian orthotopic tumor model. *Proc SPIE Int Soc Opt Eng* 2016;9788:1-15.
- Chang EY, Du J, Chung CB. UTE imaging in the musculoskeletal system. *J Magn Reson Imaging* 2015;41(4):870-883.
- Chen L, Wei Z, Chan KWY, Cai S, Liu G, Lu H, Wong PC, van Zijl PCM, Li T, Xu J. Protein aggregation linked to Alzheimer's disease revealed by saturation transfer MRI. *Neuroimage* 2019;188:380-90.
- Moon BF, Jones KM, Chen LQ, Liu P, Randtke EA, Howison CM, Pagel MD. A comparison of iopromide and iopamidol, two acidoCEST MRI contrast media that measure tumor extracellular pH. *Contrast Media Mol Imaging* 2015;10:446-55.
- Kalke RJ, Di Primio GA, Schweitzer ME. MR and CT arthrography of the knee. *Semin Musculoskelet Radiol* 2012;16:57-68.
- Yoo HJ, Hong SH, Choi JY, Lee IJ, Kim SJ, Choi JA, Kang HS. Contrast-enhanced CT of articular cartilage: experimental study for quantification of glycosaminoglycan content in articular cartilage. *Radiology* 2011;261:805-12.

20. Silvast TS, Kokkonen HT, Jurvelin JS, Quinn TM, Nieminen MT, Töyräs J. Diffusion and near-equilibrium distribution of MRI and CT contrast agents in articular cartilage. *Phys Med Biol* 2009;54:6823-36.
21. Entezari V, Bansal PN, Stewart RC, Lakin BA, Grinstaff MW, Snyder BD. Effect of mechanical convection on the partitioning of an anionic iodinated contrast agent in intact patellar cartilage. *J Orthop Res* 2014;32:1333-40.
22. Woods GW, Whelan JM. Discoid meniscus. *Clin Sports Med* 1990;9:695-706.
23. Fox AJS, Bedi A, Rodeo SA. The basic science of human knee menisci: structure, composition, and function. *Sports Health* 2012;4:340-51.
24. Gray ML, Pizzanelli AM, Grodzinsky AJ, Lee RC. Mechanical and physicochemical determinants of the chondrocyte biosynthetic response. *J Orthop Res* 1988;6:777-92.
25. Grodzinsky AJ. Electromechanical and physicochemical properties of connective tissue. *Crit Rev Biomed Eng* 1983;9:133-99.
26. Heo HY, Zhang Y, Lee DH, Jiang S, Zhao X, Zhou J. Accelerating chemical exchange saturation transfer (CEST) MRI by combining compressed sensing and sensitivity encoding techniques. *Magn Reson Med* 2017;77:779-86.
27. She H, Greer JS, Zhang S, Li B, Keupp J, Madhuranthakam AJ, Dimitrov IE, Lenkinski RE, Vinogradov E. Accelerating chemical exchange saturation transfer MRI with parallel blind compressed sensing. *Magn Reson Med* 2019;81:504-13.

Cite this article as: High RA, Ji Y, Ma YJ, Tang Q, Murphy ME, Du J, Chang EY. *In vivo* assessment of extracellular pH of joint tissues using acidoCEST-UTE MRI. *Quant Imaging Med Surg* 2019;9(10):1664-1673. doi: 10.21037/qims.2019.08.11